



High-Performance Polyethylene Fibers “Al Dente”: Improved Gel-Spinning of Ultrahigh Molecular Weight Polyethylene Using Vegetable Oils

Raphael Schaller, Kirill Feldman, Paul Smith, and Theo A. Tervoort*

Department of Materials, ETH Zurich, HCI H 513, Vladimir-Prelog-Weg 5, 8093 Zurich, Switzerland

ABSTRACT: We demonstrate that the major drawbacks of so-called gel spinning and solid-state processing of “virgin”, i.e. never molten or fully dissolved, ultrahigh molecular weight polyethylene (UHMW PE) to produce ultrahigh modulus and ultrahigh strength fibers and films, which are the unfavorably low polymer concentrations in highly flammable solvents typically employed in the former process and low production rates in the latter, can be largely avoided by employing relatively poor—as opposed to good—solvents, including, among others, fatty acids and natural oils omnipresent in, for example, fruits, nuts, and seeds, which have additional major recovery and environmental advantages.



■ INTRODUCTION

In the basic paper on the mechanism of the solution-spinning/drawing process¹—which became to be known as “gel spinning”—to create ultrahigh modulus and ultrahigh strength polyethylene fibers and films, Booij et al.² advanced the concept that the limiting factor in achieving by tensile deformation ultimate levels of extension and uniaxial alignment of weakly interacting flexible macromolecules and the, therewith, associated limiting mechanical properties is not the shape, size, or order of crystalline entities in a (semi)crystalline solid polymer such as polyethylene, but the degree at which the constituent macromolecules are entangled in it. In their experimental studies, that degree was varied by dissolving ultrahigh molecular weight polyethylene (UHMW PE) at different concentrations and consolidation through gelation the spacing between macromolecular entanglements (M_e), following the well-established concept that in solution M_e^{sol} varies as³

$$M_e^{\text{sol}} = \frac{M_e^{\text{melt}}}{\Phi} \quad (1)$$

Here M_e^{melt} represents the molecular weight between entanglements of macromolecular chains in the undiluted melt, and Φ is the polymer volume fraction in the solution. Invoking classical rubber elasticity theory,⁴ and considering entanglements trapped during the gelation event in the solid polymer to act as (semi)permanent cross-links, it follows that the maximum draw ratio λ_{max} (i.e., final/initial sample length) of a permanent network varies with the molecular weight between entanglements as

$$\lambda_{\text{max}} \propto \sqrt{M_e} \quad (2)$$

leading Booij et al.² to propose the following expression for the polymer-volume-fraction dependence of the maximum draw ratio of solution-gelled UHMW PE:

$$\lambda_{\text{max}} = \frac{\lambda_{\text{max}}^{\text{melt}}}{\sqrt{\Phi}} \quad (3)$$

Here $\lambda_{\text{max}}^{\text{melt}}$ is the maximum draw ratio of a melt-quenched solid, and as above, Φ is the polymer volume fraction in the solution that is employed to produce the fibers or films by the gel-processing route.

Thus, in order to enhance the “drawability”, i.e. increase λ_{max} of UHMW PE (typical weight-average molecular weight $\bar{M}_w \geq 3 \times 10^6$) from a value of $\lambda_{\text{max}} \approx 6$ for melt-crystallized material to a value of, for instance, a molecular draw ratio of about 50—commonly required to generate levels of stiffness in excess of 150 GPa and tensile strengths exceeding 2 GPa, a polymer solution volume fraction as low as $\Phi \approx 0.03$ would be required^{5,6}—this assuming that all entanglements present in the melt or solution are trapped.

Despite this seemingly unattractive and uneconomical process, nonetheless, ultrahigh modulus and strength UHMW PE fibers have been successfully developed on a significant commercial scale, albeit of a somewhat lower level of mechanical properties due to the higher polymer solution concentrations employed (typically $\sim 10\%$ v/v). These materials, which are sold under various trade names, including Dyneema and Spectra, today are widely employed in a broad

Received: October 7, 2015

Revised: November 10, 2015

Published: November 30, 2015

spectrum of applications ranging from bullet-proof vests to sails and ropes as well as surgical sutures (see e.g. refs 7 and 8).

Recognizing the above-described concentration issue with the solution-spinning/drawing process, Rotzinger et al.^{9–11} subsequently set out to control the entanglement density in solid UHMW PE by physicochemical means during the synthesis of the polymer, rather than the above referred semidilute solution concentration route. In their approach, conditions of the polymerization of ethylene were selected to reduce the length of the growing macromolecular chain in the fluid phase to that well below the spacing between chain entanglements found in an unperturbed polyethylene melt ($M_e = 1250$) in order to impede their formation. This was achieved by employing low polymerization temperatures, low monomer pressure, and/or low catalyst activity.^{9–11}

The polymers thus produced were compressed in the solid state, i.e., below their melting temperature—in order to maintain their low entanglement density (hence the connotation “virgin”)—into coherent films, which were subsequently drawn into ultrahigh modulus and strength fibers and films applying the usual tensile deformation techniques. Today, more than two decades after its invention,¹³ also this solvent-free process apparently is being commercialized in the form of the production of high-performance films.¹⁴

While both the “semidilute solution” and “virgin polymer” processing routes have been developed, as mentioned above, and to a certain extent have been a practical and economic success, cumbersome issues with these two technologies remain:

In the “gel-processing” method, which on the one hand is relatively forgiving from a production-control point of view, on the other hand has the significant drawback that large amounts of flammable solvent (typically 90 kg per 10 kg fiber) need to be recovered and purified, such as decalin by evaporation,¹⁵ or mineral oil extracted with, for instance, hexane or fluorocarbon compounds.¹⁶ In addition, it has been reported that the solvents and extraction means employed carry significant health hazards (ref 17 and references therein).

Although the “virgin polymer” processing route has the advantage that no solvent is employed in the film or fiber production process, it requires delicate control of both the polymerization—involving nontrivial catalyst systems—as well as of the production of solid-state compressed precursor films and relatively low rates of tensile deformation.

Accordingly, technologically attractive production of ultrahigh modulus and strength polyethylene fibers and films leaves ample room for improvement, especially as the number of beneficial applications, as well as the market as a whole, continues to expand.

In the present study, we attempted to address the above issues by exploring the concept of controlling the density of chain entanglements in solution-processed, solid UHMW PE not only simply through the volume fraction of the polymer in solution, as in the above “gel-processing” technique, but in addition by optimization of the “quality” of the solvent. As will be demonstrated below, this approach permitted us to dramatically reduce the amount of diluent required and trivialized its recovery and purification, while maintaining the flexibility of solution processing and providing an environmentally more sound approach.

N.B. It should be mentioned, of course, that exploration of diluents other than, for instance, decalin and mineral oil have been reported. For instance Motooka et al.¹⁸ described use of

aliphatic carboxylic acids, alcohols, acid amides, carboxylic acid esters, aliphatic mercaptans, aliphatic aldehydes, and aliphatic ketones to gel-process UHMW PE from solutions of relatively high polymer concentrations, but yielding disappointingly low mechanical properties of the resulting fibers, with Young's moduli invariably below 65 GPa. In addition, extraction means such as hexane, heptane, hot ethanol, chloroform, and benzene were employed with their well-known, above-referred environmental and health issues.

Rajput et al.¹⁷ attempted to dissolve 5% w/w UHMW PE in selected natural oils such as sunflower, palm (both without success), and orange oil (terpene), however, without reporting any fiber properties obtained therewith.

■ BACKGROUND

Virtually since the birth of polymer science it has been realized that fully extended and oriented macromolecular chains offer greatly enhanced mechanical properties in the orientation direction.¹⁹ In the case of flexible polymers, the most common orientation method is uniaxial solid-state plastic deformation, also known as “cold drawing”. It has been established for various polymer systems that under optimum drawing conditions (no chain-slip) the development of both Young's modulus and strength directly correlates with the applied plastic deformation.^{20–22} Assuming pseudo-affine deformation of strongly anisotropic structural “units”, Irvine and Smith⁵ were able to capture this dependence in an analytical two-parameter model, relating the Young's modulus of the oriented polymer to the plastic draw ratio λ as

$$E = \left(\frac{1}{E_u} - \left[\frac{3\lambda^3}{2(\lambda^3 - 1)} \left(1 - \frac{\arctan(\sqrt{\lambda^3 - 1})}{\sqrt{\lambda^3 - 1}} \right) - \frac{1}{2} \right] \left(\frac{1}{E_u} - \frac{1}{E_h} \right) \right)^{-1} \quad (4)$$

In this equation, the fitting parameters E_u and E_h represent the moduli of the fully unoriented and fully oriented polymer, respectively. Using this equation, the experimental “ E – λ curve” for polyethylene was accurately described using values of E_u of about 1 GPa and an oriented modulus E_h of about 300 GPa. From the experimental E – λ curve and its description using eq 4, it follows that attractive levels of stiffness in excess of 150 GPa require plastic draw ratios of more than 40. Unfortunately, the plastic draw ratio for UHMW PE, crystallized from the melt, is limited to about 6. The reason for this is that, in flexible polymers with weak interchain interactions such as polyethylene, the plastic draw ratio is believed to be limited by the same entanglements that dominate the flow behavior of polymer melts and solutions and that are trapped during solidification of the polymer system.² During “gel spinning”, the entanglement density is reduced by crystallization of UHMW PE from semidilute solutions, thereby increasing the molecular weight between entanglements and the maximum plastic draw ratio, as described by eqs 1–3.

However, eqs 1–3 assume that the macromolecular chains in solution adopt their unperturbed dimensions (theta condition). In addition, eqs 1–3 disregard the influence of the crystallization process on M_e . With respect to the first assumption, it is well established that the spatial arrangement of (flexible) macromolecules is strongly influenced by their surroundings.²³ For instance, at low polymer concentrations, in fluids that strongly interact with the polymer (“good solvents”) the radius of gyration of a coiled macromolecule is

expanded, while in a theta solvent it is equal to the state found in its molten state. Upon further reducing the solvent quality, the chains will collapse even more, accompanied by macroscopic phase separation.

The issue of chain expansion or contraction naturally impacts the entanglement density in solutions of macromolecules as well as the so-called chain “overlap” concentration, Φ^* . In polymer solutions of volume fractions below this concentration—generally referred to as “dilute” solutions—the macromolecules do not intertwine and exist as individual objects in the fluid phase. Cooling down such dilute solution to induce crystallization of the polymer, due to their non-connected nature in this phase, do not form coherent solids or gels but, rather, solidify in the form of separate crystalline entities (often single crystals). Solutions containing amounts of polymer above Φ^* , when cooled, generally solidify in the form of gels, in which the density of entanglements that existed in solution largely is preserved in the condensed phase if solidification is induced rapidly. While the quality of the solvent intuitively is of importance, it has been established that in the so-called “concentrated” regime, i.e., well above Φ^* , in polymer solutions of concentrations larger than about 10% v/v, the macromolecules adopt conformations as in the melt and in θ -solvents—also in good solvents.²⁴ That regime is, of course, precisely our object of interest, and hence, the dependence of macromolecular conformation on solvent quality may be of lesser concern.

With respect to the second assumption behind eqs 1–3, i.e. neglecting the influence of crystallization on M_w , it has been found that when the process of gelation of a solution of identical polymer concentration, or solidification of a polymer melt for that matter, occurs at elevated temperatures (lower undercooling), the maximum draw ratio of the resulting polymer solid can be drastically enhanced, likely due to (additional) disentanglement due to a macromolecular process known as “reeling in” of the polymer chains during the formation of the crystalline entities.^{2,21,25} In what follows, “undercooling” is defined in a dynamic setting, as the difference between the endset dissolution temperature, T_d , of a gel that was produced by crystallizing UHMW PE from a solvent, through cooling the solution at 10 °C/min, and the equilibrium endset dissolution temperature of UHMW PE in the same solvent, T_d^0 , obtained by a Hoffman–Weeks plot,²⁶ as is also commonly performed in polymer blends.²⁷ Unfortunately, there is no theoretical expression for the “undercooling” ($T_d^0 - T_d$) as a function of solvent quality, as the dissolution temperature T_d of the UHMW PE gel is a dynamic quantity that depends on the cooling rate that was used to produce the gel. Only the equilibrium dissolution temperature T_d^0 follows directly from the melting point depression, the latter being the difference between the equilibrium dissolution temperature of the polymer in solution, T_d^0 , and the equilibrium melting point of the pure polymer, T_m^0 , governed by the well-known equation:²⁸

$$\frac{1}{T_d^0} - \frac{1}{T_m^0} = \frac{R}{\Delta H_u} \frac{v_u}{v_1} \left((1 - \Phi) - \chi(1 - \Phi)^2 \right) \quad (5)$$

Here, R is the molar gas constant, ΔH_u is the heat of fusion per repeating unit of the polymer, v_u/v_1 is the ratio of the molar volumes of the polymer repeat unit and the solvent, $(1 - \Phi)$ is the volume fraction diluent, and χ is the Flory–Huggins interaction parameter. From this equation, it follows that the

melting point depression for a given polymer at a given volume fraction of the solvent depends on the ratio of the molar volumes of the repeating unit and the solvent and the “quality” of the solvent, given by χ . “Poor” solvents, characterized by values of χ close to 0.5 ($\chi > 0.5$ leads to phase separation), are therefore expected to crystallize at low melting point depression. Here, it should be noted that solvents that are perceived as “good” solvents for UHMW PE, such as decalin and xylene, giving rise to a more substantial melting point depression, are “athermal” at best (i.e., $\chi = 0$) due to the absence of specific interactions and typically²⁹ have values of χ upward of 0.3.

On the basis of the above, we selected the undercooling, which follows from the depression of the crystallization temperature of the polymer from solution as measured by differential scanning calorimetry (DSC) as well as solution viscosity measurements, which directly reflect coil expansion,³⁰ here in terms of melt-flow rate (MFR) as simple, but effective, tools to evaluate the physicochemical interactions between the polymer and small molecular compounds explored.

EXPERIMENTAL SECTION

Materials. Ultrahigh molecular weight polyethylene (UHMW PE; GUR4120, weight-average molecular weight $M_w = 5 \times 10^6$) was obtained from Ticona and used as received. Decahydronaphthalene (decalin; mixture of cis- and trans-isomers, Acros Organics) was dried over molecular sieves prior to use. Additional solvents, namely mineral oil (EMCplus 350, Oxiten), paraffin oil (Sigma-Aldrich), 1-dodecanol (Sigma-Aldrich), lauric acid (ABCR), stearic acid (AppliChem), peanut oil (Qualité & Prix, COOP, Switzerland), and olive oil (Filippo Berio, olio extra vergine di oliva il Classico, COOP, Switzerland) were used as received. Irganox 1010 and Irgafos 168 (BASF) were used as antioxidants.

Sample Preparation. The required amounts of UHMW PE and solvent were added to a round-bottomed flask, together with antioxidants Irganox 1010 and Irgafos 168 (both 0.5% w/w based on the UHMW PE content). The continuously stirred mixture was heated to 90 °C under nitrogen to ensure full dissolution of the antioxidant in the solvent. Approximately 6 mL of slurry was collected with a syringe and fed into a laboratory recycling twin-screw microcompounder (CPC Eindhoven, The Netherlands), operated at 120 rpm under a nitrogen blanket. The processing temperature was selected in the 160–230 °C range, depending on the diluent employed, and all solutions were mixing for at least 10 min prior to extrusion. Subsequently, the extruded strands (see Figure 1) were cooled in air to room temperature and extensively washed to extract the diluent. For instance, isopropanol and diethyl ether were used for extraction of the “green” solvents, while heptane was used for removal of paraffin oil, mineral oil and decalin.

Tensile Drawing. The washed and dried strands (typical diameter about 1.5 mm) were tensile drawn on a Kofler bench at temperatures in the 125–150 °C range. Nominal draw ratios were calculated from the displacement of ink marks printed onto the undrawn samples at 1 cm intervals.

Mechanical Properties. A paper frame was made by cutting a 70 × 10 mm² window in a light cardstock-grade (160 g/m²) paper. The stretched samples were longitudinally glued to the frame, ensuring that variation in the initial sample length of 70 mm for tensile testing was kept to a minimum. Tensile measurements were performed using an Instron 5864 static mechanical tester fitted with a 100 N load cell and equipped with mechanical clamps. A constant elongation rate of 20 mm/min, determined by the cross-head speed, was used throughout. All tests were performed at room temperature (about 23 °C). The cross-sectional area of the samples was calculated from their respective length and weight, with the latter determined using an ultramicro balance (UMT2, Mettler Toledo, Switzerland), assuming a density of 1 g/cm³. All reported values for the modulus, tensile strength, and



Figure 1. Actual extra firm strands of a gel consisting of 20% v/v UHMW PE crystallized from olive oil, nicknamed UHMW PE “Al Dente”, produced by 10 min mixing in olive oil at 230 °C, followed by extrusion and cooling in air to room temperature.

elongation at break correspond to an average of at least three separate measurements.

Thermal Analysis. Differential scanning calorimetry (DSC) was performed using a DSC 822e instrument (Mettler Toledo, Switzerland), routinely calibrated using indium standards. DSC thermograms were recorded under a nitrogen flow using 20 °C/min heating/cooling rates. Samples were heated from 25 to 180 °C and then cooled to 25 °C (two cycles were executed per sample). Typical sample weight was about 5 mg. The reported crystallization/dissolution temperatures correspond respectively to the onset/endset temperatures for the thermal transitions recorded during first-cooling/second-heating scans. The equilibrium endset dissolution temperatures of 20% v/v UHMW PE in selected solvents as well as the equilibrium endset melting temperature of UHMW PE were estimated using Hoffman–Weeks plots.²⁶ To this extent, a 20% v/v solution of UHMW PE in a given solvent was isothermally crystallized at various temperatures T_c , after which, for each crystallization temperature, the endset dissolution temperature was measured using DSC. Assuming a linear dependence of the endset dissolution temperature with the crystallization temperature, extrapolation of the endset dissolution temperatures to the line $T_d = T_c$ yields the equilibrium endset dissolution temperature T_d^0 .

Melt Flow Rate. Melt flow rates (MFR (180/10)) of solutions comprising 20% v/v UHMW PE were determined with a melt-flow index instrument (MeltFlow LT, Haake, Germany) according to the ISO1133 standard, at a temperature of 180 °C, using a weight of 10 kg. All reported values correspond to an average of seven measurements performed at 10 min collection time.

RESULTS

Thermal Analysis. In Figure 2, cooling DSC thermograms are presented of solutions comprising 20% v/v UHMW PE in a variety of liquids. Expectedly, based on respectively entropic and enthalpic effects as described by eq 5, at increasing molecular size or polarity of the solvent, the onset temperature of crystallization increased; i.e., the quality of the small molecular compounds as solvent for polyethylene decreased. Concomitantly, the temperature at which gelation occurred

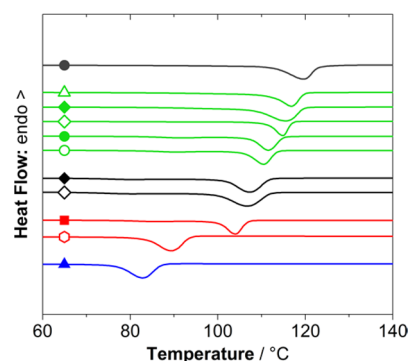


Figure 2. Cooling thermograms (not to absolute scale) of (black ●) neat UHMW PE and of 20% v/v solutions of the polymer in different solvents: (green △) peanut oil, (green ◆) olive oil, (green ◇) peanut oil–stearic acid (1:1 w/w), (green ●) stearic acid, (green ○) lauric acid, (black ◆) paraffin oil, (black ◇) mineral oil, (red ■) decalin–dodecanol (1:1 w/w), (red ◇) decalin–dodecanol (4:1 w/w), and (blue ▲) decalin.

increased. For instance, in the case of the commercially employed decalin and mineral oil, this process commenced around 88 and 113 °C, respectively, whereas in relatively poor solvents such as peanut oil and olive oil, gelation already occurred at elevated temperatures as high as about 119 °C, which is only a few degrees lower than when UHMW PE was crystallized from the melt, 122 °C. Also, of course, when a poor solvent, such as 1-dodecanol, was added to a good solvent like decalin, the temperature of the onset of crystallization/gelation rapidly increased, as illustratively shown here for a 1:1 w/w mixture of those species.

Table 1 collects an overview of the depression of the onset crystallization temperature, T_c , of reference neat UHMW PE,

Table 1. Crystallization Temperatures T_c of UHMW PE in Neat Form and Dissolved at 20% v/v in Various Solvents, Together with the Corresponding Lowering of the Crystallization Temperature, ΔT_c , Here Calculated as $\Delta T_c = T_c^{PE} - T_c$, with T_c^{PE} the Crystallization Temperature of Pure UHMW PE (122 °C)^a

polymer/solvent	T_c (°C)	ΔT_c (°C)
UHMW PE	122	
decalin	88	34
decalin:dodecanol (4:1 w/w)	94	28
decalin:dodecanol (1:1 w/w)	107	15
paraffin oil, mineral oil	112	10
lauric acid	114	8
stearic acid	115	7
stearic acid:peanut oil (1:1 w/w)	117	5
olive oil, peanut oil	119	3

^aSolvents are listed in order of decreasing ΔT_c .

and when dissolved at 20% v/v in various liquids, indicative of the “solvent quality” of the different species. As will be shown below, elevated crystallization temperatures, indicative of crystallization at low undercooling, dramatically affected the tensile deformation behavior of the solid UHMW PE produced, in line with the results reported by Smith.²⁵

To further quantify the undercooling at which the UHMW PE crystallizes during cooling, the equilibrium endset dissolution temperatures of 20% v/v UHMW PE in selected solvents were determined using Hoffmann–Weeks plots as

shown in Figure 3. Using these values, for each solvent system, the undercooling ($T_d^0 - T_d$) was calculated from the endset

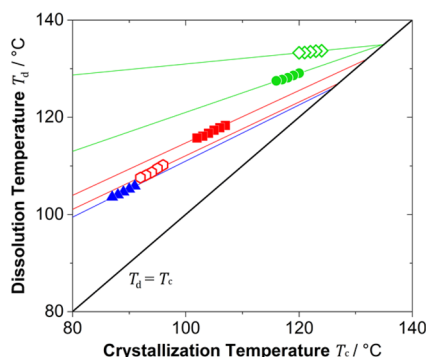


Figure 3. Hoffman–Weeks plots of 20% v/v solutions of UHMW PE in selected solvents: (green \diamond) peanut oil–stearic acid (1:1 w/w); (green \bullet) stearic acid; (red \blacksquare) decalin–dodecanol (1:1 w/w); (red \circ) decalin–dodecanol (4:1 w/w); (blue \blacktriangle) decalin. The colored lines are linear extrapolations toward the line $T_d = T_c$.

dissolution temperature T_d of UHMW PE, measured by DSC, of gels that were obtained by cooling the 20% v/v UHMW PE solutions with a rate of 20 °C/min. A plot of the undercooling as a function of the equilibrium dissolution temperature is given in Figure 4, confirming the general finding listed in Table 1,

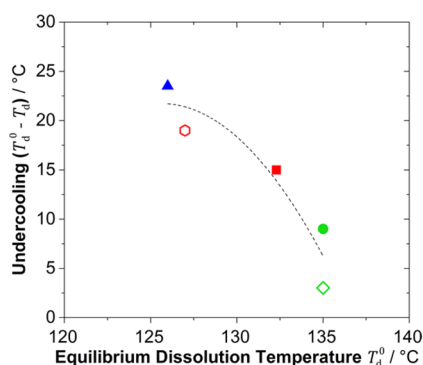


Figure 4. A plot of the undercooling ($T_d^0 - T_d$) as a function of the equilibrium dissolution temperature T_d^0 of 20% v/v solutions of UHMW PE in selected solvents: (green \diamond) peanut oil–stearic acid (1:1 w/w); (green \bullet) stearic acid; (red \blacksquare) decalin–dodecanol (1:1 w/w); (red \circ) decalin–dodecanol (4:1 w/w); (blue \blacktriangle) decalin. The dashed line is a guide for the eye only.

namely that the undercooling decreases with increasing crystallization/dissolution temperature of UHMW PE in solution. The corresponding maximum drawability λ_{\max} of fibers obtained from 20% v/v solutions of UHMW PE from the same solvents is depicted in Table 2.

Melt Flow Rate. In Table 3 are presented results of MFR tests, again of 20% v/v of UHMW PE solutions in a broad range of solvents. Evidently, the solution viscosity dramatically decreased at decreasing solvent quality—somewhat unexpectedly for such concentrated solutions (cf. ref 30). That latter result obviously is of potential advantage for gel-processing UHMW PE more efficiently.

Tensile Deformation. In the following section, the influence of the quality of the solvent on the deformation behavior of gel-processed UHMW PE will be presented.

Table 2. Comparison of Maximum Drawability λ_{\max} of the Fibers Obtained from 20% v/v Solutions of UHMW PE in Selected Solvents with the Following Thermal

Characteristics Obtained from DSC Analysis on the Gels after Extrusion: Equilibrium Dissolution Temperature T_d^0 (for Each Solvent Determined with a Hoffman–Weeks Plot;²⁶ see Figure 3), Endset Dissolution Temperature T_d , and Undercooling $\Delta T = (T_d^0 - T_d)$

solvent	T_d^0 (°C)	T_d (°C)	ΔT (°C)	λ_{\max}
decalin	126	102	24	21
decalin–dodecanol (4:1 w/w)	127	108	19	28
decalin–dodecanol (1:1 w/w)	132	117	15	34
stearic acid	135	126	9	40
stearic acid–peanut oil (1:1 w/w)	135	132	3	40

Table 3. Melt Flow Rates (MFR) of Solutions of 20% v/v UHMW PE in Different Solvents

solvent	MFR (180/10) (g/10 min)
decalin	0.1
mineral oil	2.6
decalin–dodecanol (1:1 w/w)	12.3
peanut oil	12.3
olive oil	13.5
peanut oil–stearic acid (1:1 w/w)	28.5
stearic acid	30.2

Figure 5 shows the maximum draw ratio, λ_{\max} , realized under the present conditions, as a function of the initial polymer concentration in a range of diluents, including the commercially employed decalin and mineral oil for reference purposes. As

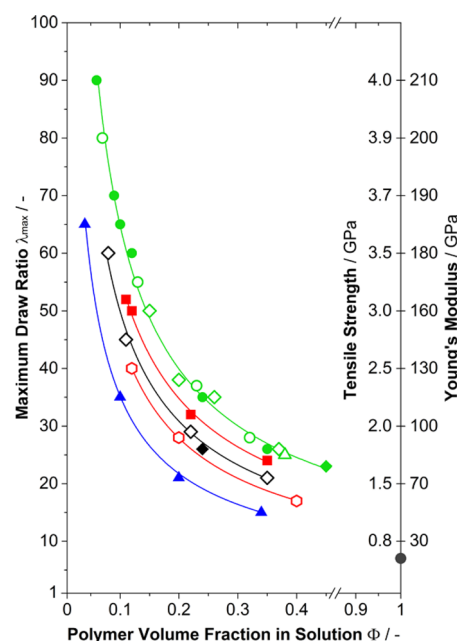


Figure 5. Maximum draw ratios and the resulting tensile strength and Young's modulus values for UHMW PE gel-processed from different solvents as a function of polymer volume fraction: (black \bullet) neat UHMW PE; (green \triangle) peanut oil; (green \blacklozenge) olive oil; (green \circ) peanut oil–stearic acid (1:1 w/w); (green \bullet) stearic acid; (green \circ) lauric acid; (black \blacklozenge) paraffin oil; (black \diamond) mineral oil; (red \blacksquare) decalin–dodecanol (1:1 w/w); (red \circ) decalin–dodecanol (4:1 w/w); (blue \blacktriangle) decalin. Lines are guides for the eye only.

clearly demonstrated with the results presented, the familiar^{1,2} dramatic increase of λ_{\max} with decreasing value of Φ was found and, therewith, increased mechanical properties (see also below). More interestingly, though, is the finding that at every concentration a significant increase in maximum draw ratio was observed for UHMW PE processed from “poor” solvents. The systematic correlation between λ_{\max} vs Φ observed for processing UHMW PE for all the solvent systems is most clearly revealed in the log–log plot presented in Figure 6. From this figure, it appears that for the range of polymer

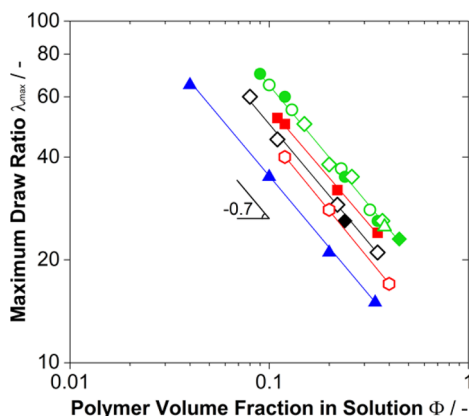


Figure 6. A log–log plot of the maximum draw ratio of UHMW PE as a function of polymer volume fraction, processed from different solvents, showing the consistent dependence of λ_{\max} on Φ due to reduction of entanglements:^{1,2} (green \triangle) peanut oil; (green \blacklozenge) olive oil; (green \diamond) peanut oil–stearic acid (1:1 w/w); (green \bullet) stearic acid; (green \circ) lauric acid; (blue \blacktriangle) decalin; (black \blacklozenge) paraffin oil; (black \diamond) mineral oil; (red \blacksquare) decalin–dodecanol (1:1 w/w); (red \circ) decalin–dodecanol (4:1 w/w). The solid lines are linear fits with a slope of -0.7 .

concentrations employed, all curves are parallel with the same slope, indicative of a multiplicative dependence of the maximum draw ratio on concentration and solvent quality, suggesting the following power-law behavior:

$$\lambda_{\max} = \frac{\lambda_{\max}^{\text{solvent}}}{\Phi^{0.7}} \quad (6)$$

Here, $\lambda_{\max}^{\text{solvent}}$ is a constant that is different for each solvent system and that is found to increase with decreasing solvent quality. Thus, it appears that the main influence of using different solvents in the gel-spinning process is the replacement of eq 3 with eq 6, as will be discussed in more detail in the Discussion section.

Mechanical Properties. While encouraged by the observed increase in “drawability” of UHMW PE processed from relatively poor solvents, this issue, of course, is whether or not this translates in similarly enhanced mechanical properties of the drawn material. That this was the case indeed is already shown in Figure 5 and is elaborated in Figure 7 (Young’s modulus, E) and Figure 8 (tensile strength). Also shown in Figure 7 is a fit of the E – λ data with eq 4, which assumes pseudoaffine deformation of the flexible polyethylene chain molecules during cold drawing, resulting in realistic values for E_u (2.4 GPa) and E_h (300 GPa), demonstrating that this relation holds independent of the quality of the solvent employed. In Figure 8 are plotted the values recorded for the tensile strength vs those for the Young’s modulus of UHMW

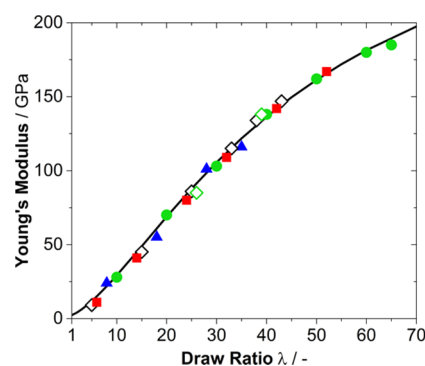


Figure 7. Development of Young’s modulus (maximum values obtained are reported) with draw ratio of UHMW PE processed from 10% v/v solutions in (green \diamond) peanut oil–stearic acid (1:1 w/w), (green \bullet) stearic acid, (blue \blacktriangle) decalin, (black \diamond) mineral oil, and (red \blacksquare) decalin–dodecanol (1:1 w/w). The curve represents the development fitted with eq 4, resulting in similar parameters according to ref 5.

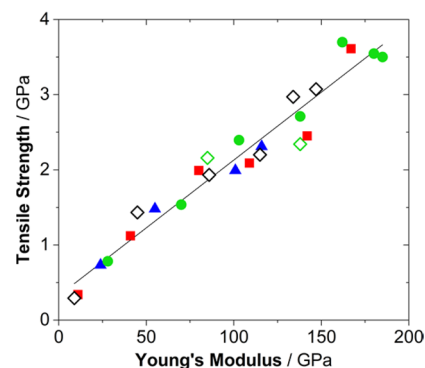


Figure 8. Tensile strength versus Young’s modulus (maximum values obtained are reported) of UHMW PE processed from 10% v/v solutions in (green \diamond) peanut oil–stearic acid (1:1 w/w), (blue \blacktriangle) stearic acid, (red \blacksquare) decalin, (black \diamond) mineral oil, and (red \blacksquare) decalin–dodecanol (1:1 w/w). The line is a guide for the eye only.

PE processed from different solvents to various draw ratios. Also here, within experimental uncertainty, no influence of solvent quality on that correlation was observed.

DISCUSSION

Mechanical Properties. The one-to-one correlations between polymer concentration and maximum draw ratio (left y-axis of Figure 5), maximum draw ratio and Young’s modulus (Figure 7), and Young’s modulus and tensile strength (Figure 8) have been condensed in Figure 5. In this figure, the corresponding Young’s modulus and tensile strength for a given maximum draw ratio are projected on the right y-axis. In this manner, Figure 5 clearly reveals the two major advantages of the use of relatively poor solvents for gel-processing UHMW PE. Those benefits are: (i) at a given polymer concentration, the material can be drawn further by as much as twice when processed from poor solvents compared to that obtained from good solvents, yielding products of correspondingly enhanced mechanical properties; (ii) when a certain set of mechanical properties is desired or sufficient for the envisaged applications, the efficiency of the solution-based gel-processing technology can be dramatically enhanced, as much higher concentrations of the polymer in poor solvents can be employed than in good solvents—by as much as a 150%.

The above advantages are illustrated graphically in Figure 9, where mechanical properties are presented of drawn UHMW

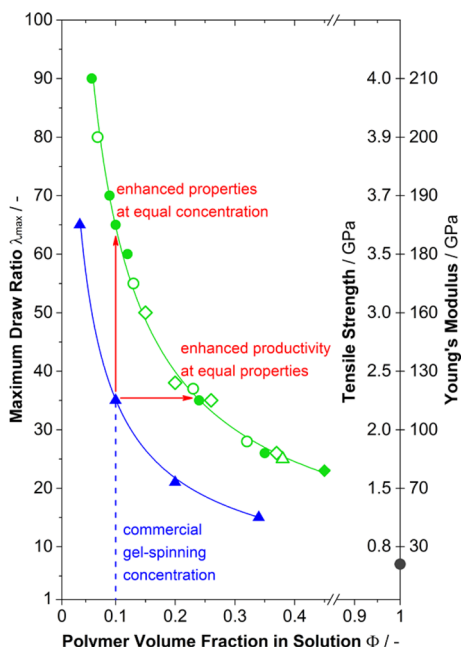


Figure 9. Maximum draw ratio with corresponding tensile strength and Young's modulus of UHMW PE gel-processed from different solvents as a function of polymer volume fraction: (black ●) neat UHMW PE; (green △) peanut oil; (green ◆) olive oil; (blue ▲) decalin; (green ◇) peanut oil–stearic acid (1:1 w/w); (green ●) stearic acid; (green ○) lauric acid. Lines are guides for the eye only.

PE processed from selected poor solvents such as stearic acid compared to the current industrial standard (good) solvent decalin.

Solvent Influence. As mentioned in the Results section, the main influence of solvent quality on the gel-spinning process is the improved maximum draw ratio upon crystallization from “poorer” solvents, embodied by replacing eq 3 with eq 6. Comparing these two equations, there are two differences: first, a change in power-law coefficient, from $\lambda_{\max} \propto \Phi^{-0.5}$ (Booij et al, eq 3) to $\lambda_{\max} \propto \Phi^{-0.7}$ (Figure 6). Second, the replacement of the constant front factor $\lambda_{\max}^{\text{melt}}$ (the maximum draw ratio of melt-crystallized UHMW PE in eq 3) with a solvent-dependent maximum draw ratio, $\lambda_{\max}^{\text{solvent}}$ in eq 6.

The change in power-law coefficient from -0.5 to -0.7 is actually in line with experimental rheological studies by Colby et al.,³⁰ who reported that the molecular weight between entanglements in solution is independent of solvent quality and scales as $M_e \propto \Phi^{-1.3}$ rather than the commonly³ used $M_e \propto \Phi^{-1}$. Substitution of $M_e \propto \Phi^{-1.3}$ into eq 2 results in $\lambda_{\max} \propto \Phi^{-0.65}$, which is close to the experimentally observed scaling $\lambda_{\max} \propto \Phi^{-0.7}$ in Figure 6.

The origin of the change in front factor is less clear. The multiplicative dependence of the maximum draw ratio on solvent quality and concentration suggests that an additional concentration-independent factor in enhanced draw ratio can be achieved by crystallization of UHMW PE from “poorer” solvents:

$$\lambda_{\max} = \frac{\lambda_{\max}^{\text{solvent}}}{\Phi^{0.7}} = \left(\frac{\lambda_{\max}^{\text{solvent}}}{\lambda_{\max}^{\text{melt}}} \right) \left(\frac{\lambda_{\max}^{\text{melt}}}{\Phi^{0.7}} \right) \quad (7)$$

The reason for the occurrence of the additional drawability factor $\lambda_{\max}^{\text{solvent}}/\lambda_{\max}^{\text{melt}}$ could be an additional degree of disentanglement induced by the crystallization process, also known as “reeling-in”. Reeling-in is found to occur more prominently during crystallization at low undercooling.^{2,21,25} Improved drawability by reeling-in can, thus, be induced in any solvent system, as was already demonstrated for crystallization of UHMW PE from decalin.²⁵ However, the rate of crystallization from moderate to good solvents becomes increasingly slow at low undercooling. This is where crystallization from poor solvents appears to be advantageous, as the poor solvent quality induces relatively fast crystallization at low undercooling, as is demonstrated experimentally in Figure 4 and Table 2, where it is shown that at an identical (realistic) cooling rate of 20 °C/min, the undercooling needed to induce crystallization of UHMW PE in “poor” solvents (high T_d^0), is lower than in “moderate” solvents (low T_d^0).

Finally, it should be noted that the “constant” factor ($\lambda_{\max}^{\text{solvent}}/\lambda_{\max}^{\text{melt}}$) appears constant for the range of concentrations studied but is expected to become unity near $\Phi \approx 1$, as then, by definition, λ_{\max} becomes equal to the maximum draw ratio of melt-crystallized material, $\lambda_{\max}^{\text{melt}}$.

Solvent Recovery. Inherent to the solution-processing/drawing technique to produce high-performance polyethylene fibers and films is, of course, the removal and recovery of the diluent that is employed to reduce the entanglement density in the solidified polymer precursor that is to be oriented by tensile deformation.

In the case of the decalin-based process, this is realized by evaporating the solvent.¹⁵ When employing mineral oils, as promoted in, for instance, the production of UHMW PE fibers by Honeywell (formerly Allied-Signal) sold under the trade name Spectra, the diluents are removed by extraction with, among others, trichlorotrifluoroethane,¹⁶ hexane, and the like. All the above species are associated with highly questionable flammable, environmental, or health issues (cf. refs 26–36 in ref 17).

In the here advanced process based on concentrated solutions in poor—as opposed to good—solvents, including, among others, fatty acids and natural oils omnipresent in, for example, fruits, nuts, and seeds, has major recovery and environmental advantages in addition to the above-described higher concentrations that can be employed to reach the required degree of disentanglement of UHMW PE, i.e., less material to recover. Furthermore, environmentally friendly extraction means can be employed to recover the solvent used in the process, which themselves can be selected to solidify for trivial recovery. An example of that case would be a mixture of stearic acid and peanut oil as the solvent and isopropanol as extraction means, or, possibly, supercritical CO₂.^{31,32}

CONCLUSIONS

The results presented here clearly indicate the major benefits of employing poor—as opposed to good—solvents in the gel-processing method, as substantially higher initial polymer concentrations can be applied, therewith drastically reducing the solvent recovery needs, not to mention the environmental gains of many of the systems described.

AUTHOR INFORMATION

Corresponding Author

*E-mail: theo.tervoort@mat.ethz.ch (T.A.T.).

Notes

The authors declare no competing financial interest.

■ ACKNOWLEDGMENTS

The authors express their gratitude to Prof. Piet Lemstra and Bob Fifield for stimulating discussions.

■ REFERENCES

- (1) Smith, P.; Lemstra, P. J. *J. Mater. Sci.* **1980**, *15* (2), 505–514.
- (2) Smith, P.; Lemstra, P. J.; Booij, H. C. *J. Polym. Sci., Polym. Phys. Ed.* **1981**, *19* (5), 877–888.
- (3) Graessley, W. W. *Adv. Polym. Sci.* **1974**, *16*, 1–179.
- (4) Treloar, L. R. G. *The Physics of Rubber Elasticity*, 3rd ed.; Clarendon Press: Oxford, UK, 2005.
- (5) Irvine, P. A.; Smith, P. *Macromolecules* **1986**, *19* (1), 240–242.
- (6) Smith, P.; Lemstra, P. J.; Pijpers, J. P. L. *J. Polym. Sci., Polym. Phys. Ed.* **1982**, *20* (12), 2229–2241.
- (7) Homepage Dyneema; <http://www.dyneema.com> (accessed Aug 27, 2015).
- (8) Homepage Honeywell Advanced Fibers and Composites; <http://www.honeywell-advancedfibersandcomposites.com> (accessed Aug 27, 2015).
- (9) Rotzinger, B. P.; Chanzy, H. D.; Smith, P. *Polymer* **1989**, *30* (10), 1814–1819.
- (10) Smith, P.; Chanzy, H. D.; Rotzinger, B. P. *Polym. Commun.* **1985**, *26* (9), 258–260.
- (11) Smith, P.; Chanzy, H. D.; Rotzinger, B. P. *J. Mater. Sci.* **1987**, *22* (2), 523–531.
- (12) Raju, V. R.; Rachapudy, H.; Graessley, W. W. *J. Polym. Sci., Polym. Phys. Ed.* **1979**, *17* (7), 1223–1235.
- (13) Chanzy, H.; Rotzinger, B.; Smith, P. U.S. Patent 5,036,148, July 30, 1991.
- (14) Homepage Teijin Endumax; <http://www.teijinendumax.com> (accessed Aug 27, 2015).
- (15) Smith, P.; Lemstra, P. J. U.S. Patent 4,344,908, Aug 17, 1982.
- (16) Prevorsek, D. C.; Kavesh, S. U.S. Patent 4,413,110, Nov 1, 1983.
- (17) Rajput, A. W.; Aleem, A. u.; Arain, F. A. *Int. J. Polym. Sci.* **2014**, *2014*, 1–5.
- (18) Motooka, M.; Mantoku, H.; Yagi, K.; Takimoto, K. U.S. Patent 5,055,248, Oct 8, 1991.
- (19) Carothers, W. H.; Hill, J. W. *J. Am. Chem. Soc.* **1932**, *54* (4), 1579–1587.
- (20) Capaccio, G.; Crompton, T. A.; Ward, I. M. *J. Polym. Sci., Polym. Phys. Ed.* **1976**, *14* (9), 1641–1658.
- (21) Capaccio, G.; Ward, I. M. *Polymer* **1975**, *16* (4), 239–243.
- (22) Capaccio, G.; Ward, I. M. *Polymer* **1974**, *15* (4), 233–238.
- (23) de Gennes, P.-G. *Scaling Concepts in Polymer Physics*; Cornell University Press: London, UK, 1979.
- (24) Cheng, G.; Graessley, W.; Melnichenko, Y. *Phys. Rev. Lett.* **2009**, *102* (15), 157801.
- (25) Smith, P. *Macromolecules* **1983**, *16* (11), 1802–1803.
- (26) Hoffman, J. D.; Weeks, J. J. *J. Res. Natl. Bur. Stand., Sect. A* **1962**, *66A* (1), 13–28.
- (27) Nishi, T.; Wang, T. T. *Macromolecules* **1975**, *8* (6), 909–915.
- (28) Flory, P. J. *J. Chem. Phys.* **1949**, *17* (3), 223–240.
- (29) Milner, S. T.; Lacasse, M.-D.; Graessley, W. W. *Macromolecules* **2009**, *42* (3), 876–886.
- (30) Colby, R. H.; Fetters, L. J.; Funk, W. G.; Graessley, W. W. *Macromolecules* **1991**, *24* (13), 3873–3882.
- (31) Hobbs, T.; Lesser, A. J. In *Drawing of Nylon 6,6 and Ultrahigh Molecular Weight Polyethylene Fibers in Supercritical CO₂*, 58th Annual Technical Conference of the Society-of-Plastics-Engineers, Orlando, FL, SPE, Ed.; Technomic Publ. Co. Inc.: Lancaster, PA, 2000; pp 1705–1709.
- (32) Zhang, J.; Busby, A. J.; Roberts, C. J.; Chen, X.; Davies, M. C.; Tendler, S. J. B.; Howdle, S. M. *Macromolecules* **2002**, *35* (23), 8869–8877.